Journal of Applied Physics ARTICLE scitation.org/journal/jap

Propagating spin-wave spectroscopy in a liquid-phase epitaxial nanometer-thick YIG film at millikelvin temperatures

Cite as: J. Appl. Phys. **133**, 143905 (2023); doi: 10.1063/5.0137437
Submitted: 2 December 2022 · Accepted: 21 February 2023 ·
Published Online: 11 April 2023

View Online Export Citation CrossMark

Sebastian Knauer,[1,a)] Kristýna Davídková,[2] David Schmoll,[1,3] Rostyslav O. Serha,[1,3] Andrey Voronov,[1,3] Qi Wang,[1] Roman Verba,[4] Oleksandr V. Dobrovolskiy,[1] Morris Lindner,[5] Timmy Reimann,[5] Carsten Dubs,[5] Michal Urbánek,[2] and Andrii V. Chumak[1]

AFFILIATIONS

[1]Faculty of Physics, University of Vienna, A-1090 Vienna, Austria
[2]CEITEC BUT, Brno University of Technology, 612 00 Brno, Czech Republic
[3]Vienna Doctoral School in Physics, University of Vienna, A-1090 Vienna, Austria
[4]Institute of Magnetism, Kyiv 03142, Ukraine
[5]INNOVENT e.V. Technologieentwicklung, Prüssingstraße 27B, 07745 Jena, Germany

Note: This paper is part of the Special Topic on: Recent Advances in Magnonics.
[a)]**Author to whom correspondence should be addressed:** knauer.seb@gmail.com

27 July 2023 11:04:24

ABSTRACT

Performing propagating spin-wave spectroscopy of thin films at millikelvin temperatures is the next step toward the realization of large-scale integrated magnonic circuits for quantum applications. Here, we demonstrate spin-wave propagation in a 100 nm-thick yttrium-iron-garnet (YIG) film at temperatures down to 45 mK, using stripline nanoantennas deposited on YIG surface for electrical excitation and detection. The clear transmission characteristics over the distance of 10 μm are measured and the extracted spin-wave group velocity and the YIG saturation magnetization agree well with the theoretical values. We show that the gadolinium-gallium-garnet (GGG) substrate influences the spin-wave propagation characteristics only for the applied magnetic fields beyond 75 mT, originating from a GGG magnetization up to 62 kA/m at 45 mK. Our results show that the developed fabrication and measurement methodologies enable the realization of integrated magnonic quantum nanotechnologies at millikelvin temperatures.

© 2023 Author(s). All article content, except where otherwise noted, is licensed under a Creative Commons Attribution (CC BY) license (http://creativecommons.org/licenses/by/4.0/). https://doi.org/10.1063/5.0137437

I. INTRODUCTION

Yttrium-iron-garnet (YIG, $Y_3Fe_5O_{12}$) is the ideal choice of material to build and develop classical and novel quantum technologies[1,2] by coupling spin waves, and their single quanta magnons, to phonons,[3] fluxons,[4] or to microwave and optical photons.[5–8] These technologies may be realized by the coupling to bulk or spherical YIG samples (e.g., Refs. 9 and 10) or by the fabrication of integrated structures in thin YIG films.[11,12] Such nanometer-thick films can be grown using liquid-phase epitaxy (LPE),[13,14] exhibiting long spin-wave propagation lengths, narrow linewidths, and low damping constants.[13–16] Significant progress was made in realizing YIG nano-waveguides with lateral dimensions down to 50 nm,[11] in understanding the spin-wave properties in these waveguides,[17] and in using them for room temperature data processing.[12]

To create, propagate, and read out spin waves at a single magnon level, millikelvin temperatures are required to suppress thermal magnons according to the Bose–Einstein statistics. Using Bose–Einstein statistics, one can estimate that, for example, at a temperature of 100 mK and 10 GHz, the thermal magnon population is about 0.01.[2] The established technique of ferromagnetic resonance (FMR) spectroscopy was used to characterize YIG films of micrometer[18] and nanometer thicknesses[19–21] at kelvin temperatures. At millikelvin temperatures, FMR measurements were performed on micrometer[22] and nanometer-thick[19–21] YIG films.

© Author(s) 2023

Another method, propagating spin-wave spectroscopy (PSWS), is often used to characterize magnon transport between spatially-separated sources and detectors. This technique was successfully used in thin films at room[23–25] and near room temperature,[26] and at millikelvin temperatures for micrometer-thick YIG slabs[27,28] and micrometer-scaled hybrid magnon-superconducting systems.[29]

The ability to process information in sub-100 nm sized magnonic structures is one of the key advantages of magnonics, which translates also to the fields of hybrid opto-magnonic quantum systems and quantum magnonics. To couple PSW to these nanostructures efficiently at millikelvin temperatures, integrated nanoantennas[24,30] are required. Here, we demonstrate PSWS at millikelvin temperatures, with base temperatures reaching 45 mK in a 100 nm-thick YIG film, using integrated nanoantennas separated by 10 μm for excitation and detection. The analysis is focused on magnetostatic surface spin waves (MSSWs, also called "Damon–Eshbach" mode) that propagate perpendicular to an in-plane magnetic field $\mathbf{k} \perp \mathbf{B}$. We find that magnon transport at the nanometer structure scale can be measured also down to millikelvin temperatures. Although the propagation signal is measurable across a wide field and temperature range, we observe that the transmitted signal is distorted for applied magnetic fields above 75 mT. This effect is largely caused by the magnetization of the gadolinium-gallium-garnet (GGG) substrate, on which the YIG film is grown. It reaches 47 kA/m for 75 mT of applied external magnetic field at 45 mK temperature. In general, our findings agree with the increase in the damping of YIG grown on GGG at low temperatures reported in the literature.[19–22] First, we explain the sample preparation and experimental techniques, before we continue to pre-characterize the sample at room and base temperature, using standard FMR techniques. Then, we discuss the first PSWS experiment, in which a fixed external magnetic field is applied and the temperature is swept from base to room temperature. We continue to analyze the propagation characteristics in more detail by comparing the low temperature measurements to room temperature results and extract the spin-wave group velocities. Finally, we perform PSWS at higher external magnetic fields to investigate the propagation characteristics between the room and base temperature. The magnetization of GGG is measured by vibrating sample magnetometry (VSM) of a GGG-only substrate at low temperatures.

II. SAMPLE AND EXPERIMENTAL SETUPS

In our experiments, we use an LPE-grown 100 nm-thick (111)-orientated YIG film on a 500 µm-thick GGG substrate, as sketched in Fig. 1(a). Atop the YIG film, we fabricate nanoantennas connected to CPWs, using an electron-beam lithography process [Fig. 1(b)].

First, a single layer of PMMA is spin-coated and baked. To avoid charging effects, we use about a 4 nm layer of conductive coating on top of the PMMA. After, we use electron-beam lithography to write the antenna structures, develop the sample, and deposit a layer of Ti(5 nm)/Au(55 nm), using electron-beam physical vapor deposition, followed by lift-off. Figure 1(c) shows an optical (top) and a secondary-electron image (bottom) with the coplanar waveguides and stripline nanoantennas used in this work. Here, the nanoantennas have a spacing of 10 µm. The stripline nanoantennas possess a width of 330 nm and a length of 120 µm. Additionally, we fabricate a reference coplanar waveguide to measure the FMR signals only [see Fig. 1(a)]. After fabrication, the sample is glued and then wire-bonded, with a 75 µm diameter gold wire, to a high-frequency printed circuit board and mounted into the dilution refrigerator.

Our setup is based on a cryogenic-free dilution refrigerator system (Bluefors-LD250), which reaches base temperatures below 10 mK at the mixing chamber stage. The sample space possesses a base temperature of about 16 mK. During operation, the sample space heats up to about 45 mK. At these temperatures, the thermal

27 July 2023 11:04:24

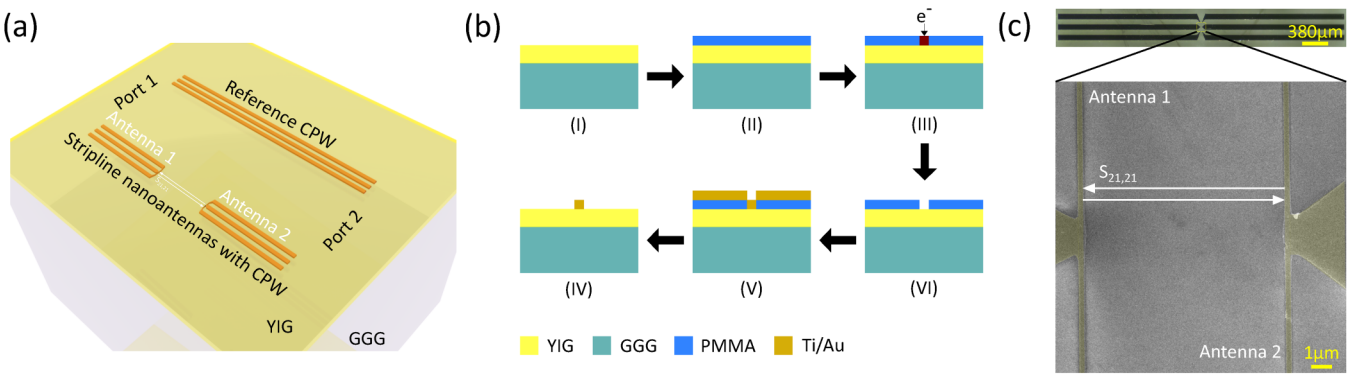


FIG. 1. Overview of the electron-beam lithographed stripline nanoantennas on the yttrium-iron-garnet film. (a) Sketch of the sample used in these measurements. Stripline nanoantennas coupled to coplanar waveguide (CPW) and the reference CPW are fabricated atop a 100 nm-thick yttrium-iron-garnet film on a 500 µm-thick gadolinium-gallium-garnet substrate. (b) The coplanar-waveguide coupled nanoantennas are fabricated with electron-beam lithography. These nanoantennas are made of Ti(5 nm)/Au(55 nm) (more details in the main text). (c) Optical and secondary-electron images of the CPW nanoantennas used in the manuscript. These nanoantennas are 10 µm spaced apart and have a width of 330 nm and a length of 120 µm. The propagating spin waves (PSWs) are excited and detected by the stripline nanoantennas 1 and 2, respectively. The transmission is measured through the S-parameters, acquired by a vector network analyser.

© Author(s) 2023

excitations of gigahertz-frequency magnons and phonons are still suppressed.[2] The input signal is transmitted and collected from the sample [ports 1 and 2 Fig. 1(a)], using high-frequency copper and superconducting wiring each attenuated by 7 dB to reduce thermal noise. The signals are collected with a 70 GHz vector network analyser (Anritsu VectorStar MS4647B).

The room temperature measurements are carried out on a home-built setup. The setup consists of a VNA (Anritsu MS4642B) connected to an H-frame electromagnet GMW 3473-70 with an 8 cm air gap for various measurement configurations and magnet poles of 15 cm diameter to induce a sufficiently uniform biasing magnetic field. The electromagnet is powered by a bipolar power supply BPS-85-70EC (ICEO), allowing it to generate up to 0.9 T at 8 cm air gap. The input powers are adjusted to obtain the same power levels at the sample as in the cryogenic measurements, to account for cable losses and the previously mentioned attenuators, not including impedance mismatches that one may encounter from temperature changes. The microwave powers for each individual experiment are stated later. However, we note that the comparison of transmission magnitudes between room and low temperatures can only show qualitative trends, as it is beyond the scope of the experiments to fully impedance match (temperature-dependent) cryogenic setups, CPWs, and nanoantennas.

III. RESULTS AND DISCUSSION

First, we use the reference CPW to pre-characterize the sample and to estimate the Gilbert damping α_s.

We plot our FMR and PSWS data according to

$$S'_{21}(f) = \frac{S_{21,\mathrm{sig}}(f) - S_{21,\mathrm{ref}}(f)}{S_{21,\mathrm{ref}}(f)}, \tag{1}$$

where f denotes the set of frequency points of the complex transmission signal $S_{21,\mathrm{sig}}(f)$ and reference $S_{21,\mathrm{ref}}(f)$ values.[31] The reference signal is obtained by detuning the external magnetic field to ensure that the resonance feature is outside the frequency range of interest (typical detuning +50 or +100 mT). For the FMR reference measurements, we find the Gilbert damping parameter $\alpha_s = (5.1 \pm 0.3) \times 10^{-4}$ for room temperature and $\alpha_s = (3 \pm 1.5) \times 10^{-3}$ at 45 mK, respectively. The large error in the low temperature case originates from the fit uncertainty in the slope of FMR linewidth vs FMR frequency (see Sec. A in the supplementary material). The methodology developed in Ref. 31, which accounts for asymmetry and phase offset in the distorted FMR signal, was used. The Gilbert damping at room temperature is in good agreement with measurements performed on a bare (non-lithographed)

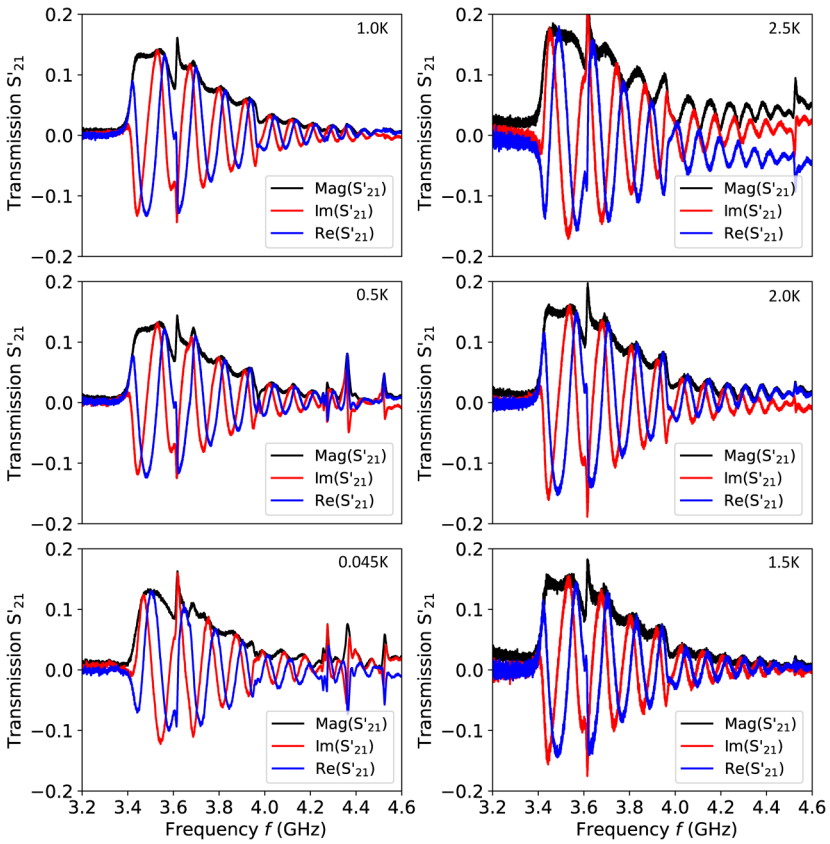


FIG. 2. Linear magnitude, real, and imaginary part of the S'_{21} parameters for propagating spin waves (PSW) in the Damon–Eshbach mode, using 50 mT of external magnetic field and different temperatures. The applied microwave power was set to −28 dBm (at the sample) with an average sampling of 50 for 45 mK–1 K and 100 for 1.5–2.5 K. The FMR point ($k = 0$) is constant at 3.36 GHz (189 kA/m) for all measured PSW.

27 July 2023 11:04:24

© Author(s) 2023

sample, using a physical property measurement system (Sec. A in the supplementary material), accounting for metallization effects in the lithography process. The obtained values are also in good agreement with previous measurements of continuous, non-structured YIG films.[32–34] The value obtained at 45 mK agrees in the order of magnitude with previously reported values for thin YIG films at kelvin temperatures.[19] For more details, see Sec. A in the supplementary material.

We perform the first PSWS experiment at a fixed external magnetic field of 50 mT, using the stripline nanoantennas shown in Fig. 1. Figure 2 displays the linear magnitude (black), real (blue), and imaginary (red) part of the transmission data (cw-mode), together with a temperature sweep from the base temperature of 45 mK up to 2.5 K, i.e., about the Curie–Weiss temperature of GGG.[35,36] The spin waves are excited with a power of −28 dBm at the sample, with the external magnetic field applied perpendicular

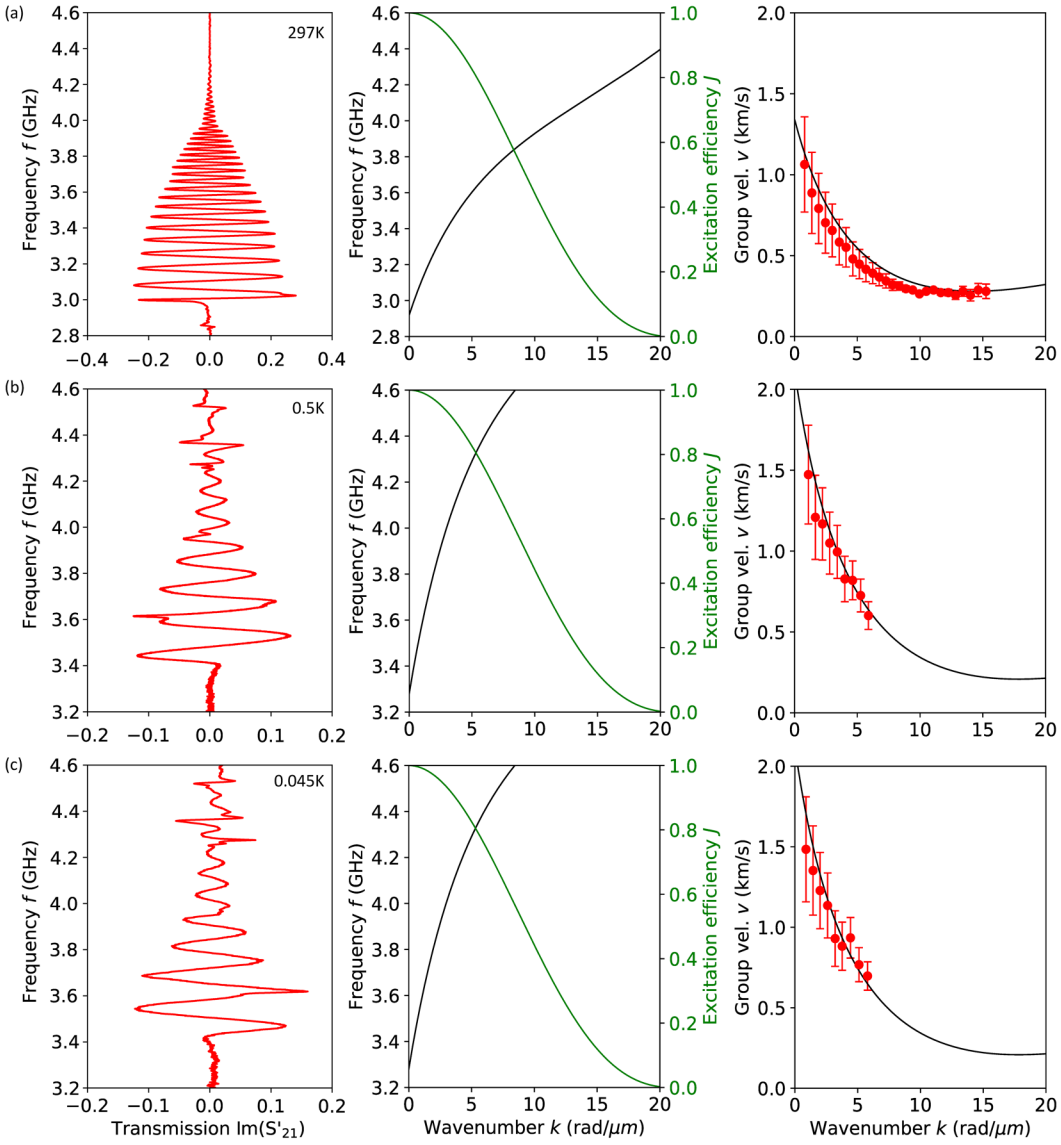


FIG. 3. Imaginary part of the S'_{21} parameter, calculated dispersion relation, antenna excitation efficiency, and group velocity for PSW (Damon–Eshbach mode), using 50 mT external field at different temperatures. The theoretical group velocity is calculated as the derivation of the dispersion relation and measured as $v_g = \delta f \cdot D$, with the periodicity of the transmission in the $\mathrm{Im}(S'_{21})$ parameters δf and the gap between the nanoantennas D (see Ref. 23). The parameters measured and used for the calculation are the following: (a) 297 K, $M_s = 142\,\mathrm{kA/m}$, (b) 500 mK, $M_s = 189\,\mathrm{kA/m}$, and (c) 45 mK, $M_s = 189\,\mathrm{kA/m}$. The effective saturation magnetization increases and thus group velocity increases by about 50% at millikelvin temperatures.

27 July 2023 11:04:24

© Author(s) 2023

to the propagation direction. In Fig. 2, we verify the ability to measure the transmission across the entire temperature range and observe a propagation signal with a fixed FMR point ($k = 0$) of about 3.36 GHz, corresponding to an effective saturation magnetization (including cubic anisotropy) of about 189 kA/m. This value agrees well with the theoretical expectation of about 196 kA/m, considering YIG film thickness, fabrication-induced damage, and the influence of the GGG substrate on the magnetization of YIG (see Sec. B in the supplementary material). The signal amplitude increases by about 30% from 45 mK to 2.5 K. This behavior points to changes in Gilbert damping, group velocity, or impedance. We note, that some of the additional resonance features in these and the following measurements may originate from reflections in impedance mismatch or vibration noise at cryogenic temperatures.

We continue to investigate the spin-wave propagation in more detail and compare the results to room temperature measurements. Figure 3 (first column) depicts the imaginary part of the S'_{21} parameters for PSWs between the two nanoantennas at three different selected temperatures: (a) 297 K, (b) 500 mK, and (c) 45 mK, at a fixed external magnetic field of 50 mT. The second column in Fig. 3 shows the corresponding calculated dispersion relations for MSSWs (black), using the Kalinikos–Salvin model,[37] with an exchange constant of $A_{YIG} = 3.6 \times 10^{-12}$ J/m, and gyromagnetic ratio $\gamma_{YIG}/2\pi = 28$ G Hz/T. The maximum excitation efficiency J (green line Fig. 3) is governed by the 330 nm stripline nanoantennas.[23] The third column in Fig. 3 shows the theoretical group velocities as the derivation of the dispersion relation (black curve) and the measured values given by $v_g = \delta f \cdot D$ (red dots), where δf is the frequency spacing between two neighboring oscillation maxima/minima in the frequency points of the $\mathrm{Im}(S'_{21})$ parameters and D the gap between the nanoantennas.[23] The corresponding wavenumber is recalculated for each given frequency, using the Kalinikos–Salvin model. The errors in the calculated group velocities are estimated from the error propagation of the derivative in the frequency reading. We observe a reduction in propagation amplitude by about 50% between the room and both cryogenic temperatures caused by the increase in Gilbert damping. We find values for the effective saturation magnetization of $M_s = 142$ kA/m at room temperature and $M_s = 189$ kA/m for 45 and 500 mK. The constant effective saturation magnetization at millikelvin temperatures is in good agreement with the literature,[38,39] with a value close to the observed ones in micrometer-thick YIG samples.[27] In accordance with the increase in effective saturation magnetization, we observe an increase in the group velocity by about 50%. The measured values are in good agreement with the theoretically calculated group velocities.

We continue our investigations by comparing the spin-wave propagation for higher external magnetic fields than in the previous measurements, at 297 K [Fig. 4(a)] and 45 mK [Fig. 4(b)]. Figure 4 shows the linear magnitude (black), real (blue), and imaginary (red) part for PSW in the Damon–Eshbach mode at selected magnetic fields. At room temperature, we measure the spin-wave signal over a wide external magnetic field range up to about 900 mT. Examples for low fields are given in Fig. 4(a). However, at 45 mK, the propagation characteristics are changing [Fig. 4(b)]. After about 75 mT, the magnitude of the spin-wave signal is reduced significantly and only a signature in the oscillation behavior can be observed. Moreover, the fixed phase relation between the imaginary and real parts disappears, causing challenges in plotting the linear magnitude of the propagation signal. Examples for the reduced spin-waves signals are given for 175 and 200 mT. This opposing behavior between the room and base temperature is a clear indication, that beyond an external field of about 75 mT the GGG substrate magnetizes enough to influence the propagation characteristics of the spin waves. Thus, future millikelvin measurements at high magnetic fields may rely on suspended YIG

27 July 2023 11:04:24

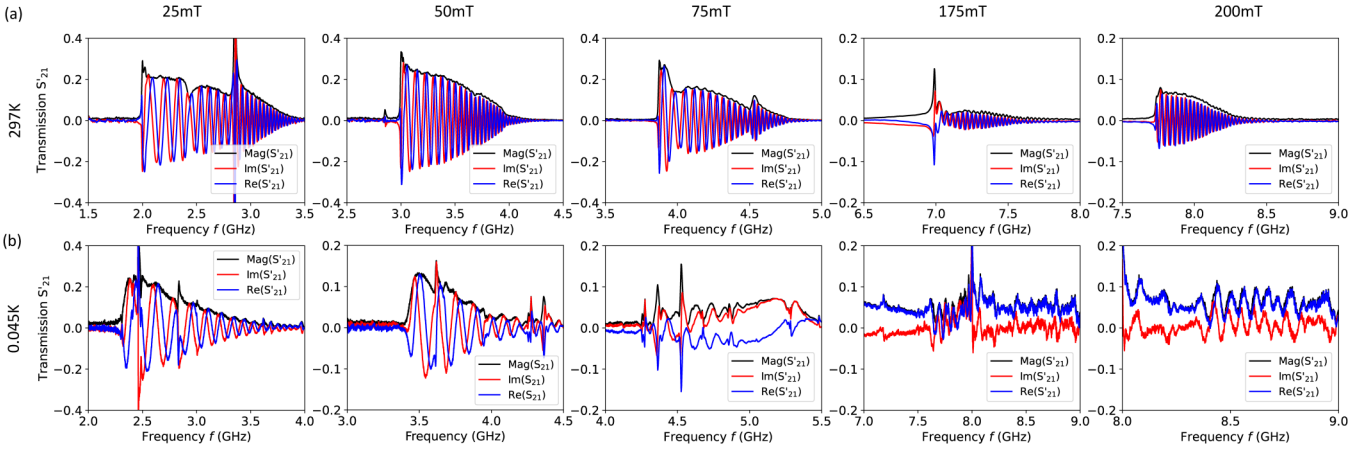


FIG. 4. Linear magnitude, real, and imaginary part of the S'_{21} parameters for PSWS in the Damon–Eshbach mode at different external fields. The applied microwave power was set to −28 dBm (at the sample) with an average of 10 (for 297 K) and 25 (for 0.045 K). (a) Room temperature (297 K): The spin-wave propagation can be measured over a wide magnetic field range. (b) Base temperature (45 mK): The spin-wave propagation for magnetic fields in the range from about 25 to 75 mT is trackable, while above 75 mT the magnitude and its propagation characteristics start to be distorted. This effect is a result of the increased magnetization of the GGG substrate (see Fig. 5).

© Author(s) 2023

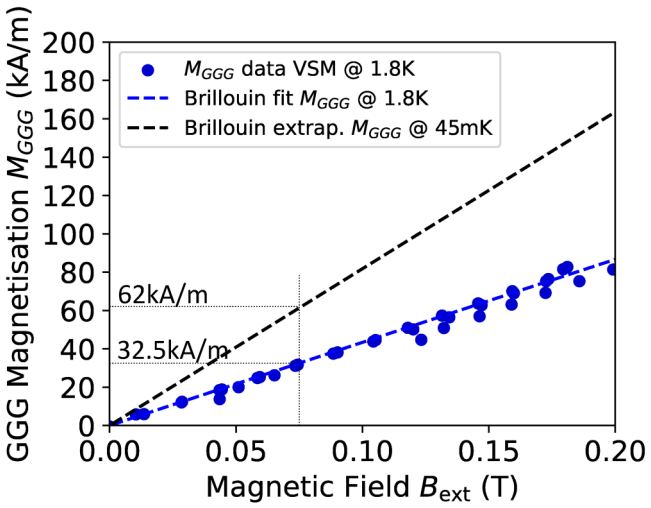


FIG. 5. Magnetization of the GGG substrate vs the applied magnetic field. A GGG-only sample is measured, using a vibrating sample magnetometer (VSM) at 1.8 K (dark-blue dots), leading, for example, to an effective magnetization of 32.5 kA/m at 75 mT. The data are in good agreement with the Brillouin fit (blue dashed line). For more information, see Sec. C in the supplementary material. From these data, the magnetization values for 45 mK are extrapolated, using the Brillouin function (black dashed line). At 75 mT, the magnetization increases to about 62 kA/m.

membranes or triangular nanostructures, which have already been demonstrated in other material systems (e.g., Ref. 40). To estimate the influence of the paramagnetic GGG substrate on the spin-wave propagation in YIG, we conclude our investigations by measuring the GGG magnetization M_{GGG} of a $4 \times 4 \times 0.5$ mm GGG-only substrate, using a vibrating sample magnetometer (VSM) in the temperature range from 1.8 to 300 K, in the presence of fields of up to 9 T. The results at 1.8 K for our magnetic fields of interest are shown in Fig. 5 (dark-blue dots). Using Brillouin formalism (see Sec. C in the supplementary material), we find a good agreement between measurement results and data. As the VSM is limited to kelvin temperatures, we extrapolate the magnetization values for GGG at 45 mK (black dashed line). For example, at 75 mT (Fig. 5 black dots) we find, that GGG possesses a magnetization value of 32.5 kA/m at 1.8 K, which increases to about 62 kA/m at 45 mK. Thus, the temperature and magnetic field dependent GGG magnetization may explain the observed reduction in the PSW amplitudes and the propagation distortions above external magnetic fields of 75 mT. Our results are consistent with previous investigations in the magnetization interaction between YIG and GGG.[41,44]

However, the role of the paramagnetic GGG substrate on spin waves in YIG is the subject of separate systematic studies. Our PSWS measurements, supported by the FMR and VSM studies, suggest that the magnetic moment induced in GGG at millikelvin temperatures by the application of relatively large magnetic fields is at least partly responsible for the increase in spin-wave damping. The increase in the Gilbert damping constant α can only be approximately quantified, as this requires plotting the FMR linewidth ΔB against the FMR frequency f_{FMR} over a wide range of applied fields. However, since the FMR linewidth depends on the degree of the magnetization of the GGG (given by the temperature and the applied field—see Fig. 5), the dependence $\Delta B(f_{FMR})$ becomes nonlinear and the parameter α loses its original physical meaning. Moreover, the measurement of FMR on nanometer-thick samples requires the careful subtraction of the reference microwave transmission signal [see Eq. (1)] at a 50 mT detuned magnetic field. Since this reference signal also depends significantly on the GGG magnetization at low temperatures, the measurement uncertainties increase. Nevertheless, we can conclude that the increase in spin-wave damping in the nanometer-thick YIG films on GGG contributes to the previously reported increase in damping in the micrometer-thick films on GGG.[18,19,22] Other phenomena that could contribute to the distortion of the PSWS experiments at the nanoscale at fields above 75 mT are the possible dependence of the magnetocrystalline anisotropy, caused by the dependence of the cubic crystalline anisotropy of YIG and the stress-induced anisotropy of the YIG/GGG lattice mismatch on temperature, and the absorption/distortion of the microwave signal in the CPW transmission lines [see Fig. 1(a)] by the magnetized GGG substrate.

IV. CONCLUSIONS

In conclusion, we have shown for the first time that propagating spin-wave spectroscopy in 100 nm-thin YIG films can be performed in a wide temperature range, from millikelvin to room temperature, while tracking the spin-wave propagation characteristics. At a fixed external magnetic field of 50 mT, we confirm that the propagating spin waves maintain a constant ferromagnetic resonance frequency below temperatures of about 2.5 K. However, we observe that the signal amplitude increases by 30% between 45 mK and 2.5 K and further by about 50% when the temperature is raised to room temperature, pointing to changes in Gilbert damping, group velocity, or impedance. In contrast to previous work, we demonstrate that only beyond an external field of about 75 mT the GGG substrate magnetizes up to 62 kA/m and influences the spin-wave propagation at low temperatures. With our experiments, we illustrate that although the GGG substrate changes the spin-wave propagation characteristics at millikelvin temperatures, future large-scale integrated YIG nanocircuits can be realized and measured.

SUPPLEMENTARY MATERIAL

See the supplementary material for Kittel and Gilbert measurements and fits of the pre-characterization experiment, the theoretical temperature dependence of the YIG magnetization, and the temperature dependence of the GGG magnetization.

ACKNOWLEDGMENTS

The authors thank Vincent Vlaminck for useful discussions and feedback. S.K. acknowledges the support by the H2020-MSCA-IF under Grant No. 101025758 (OMNI). K.D. was supported by the Erasmus+ program of the European Union. The authors acknowledge CzechNanoLab Research Infrastructure supported by MEYS CR (LM2018110). A.V.C. acknowledges the support by the Austrian Science Fund (FWF) through Project No. I 4696-N. The work of C.D. was supported by the Deutsche

27 July 2023 11:04:24

© Author(s) 2023

Forschungsgemeinschaft (DFG, German Research Foundation) under Grant No. 271741898. The work of M.L. was supported by the German Bundesministerium für Wirtschaft und Energie (BMWi) under Grant No. 49MF180119. O.V.D. acknowledges support by the Austrian Science Fund (FWF) under Grant No. I 6079-N (FluMag). C.D. thanks O. Surzhenko and R. Meyer (INNOVENT) for their support.

Author Declarations

Conflict of Interest

The authors have no conflicts to disclose.

Author Contributions

S.K. and M.U. conceived the experiment in discussion with A.V.C.
S.K. and K.D. performed the experiments under the guidance of M.U. and A.V.C.
S.K. and K.D. analyzed and interpreted the data with support from A.V.C.
R.O.S. and O.V.D. performed the VSM measurements at kelvin temperatures.
A.V. simulated the influence of the GGG substrate.
M.L. and T.R. prepared the LPE sample. C.D. conceived and supervised the LPE film growth.
Q.W. and R.V. supported the measurements with theoretical expertise. D.S. and S.K. set up the cryogenic system. R.S. supported the measurements and analysis of the measurements.
S.K. wrote the manuscript with support from all co-authors.

Sebastian Knauer: Conceptualization (lead); Formal analysis (lead); Funding acquisition (equal); Investigation (lead); Project administration (equal); Resources (equal); Visualization (lead); Writing – original draft (lead); Writing – review & editing (equal). **Kristýna Davídková:** Formal analysis (lead); Investigation (lead); Visualization (supporting); Writing – review & editing (equal). **David Schmoll:** Resources (equal); Writing – review & editing (supporting). **Rostyslav O. Serha:** Investigation (supporting); Writing – review & editing (supporting). **Andrey Voronov:** Formal analysis (supporting); Writing – review & editing (supporting). **Qi Wang:** Formal analysis (supporting); Writing – review & editing (supporting). **Roman Verba:** Formal analysis (supporting). **Oleksandr V. Dobrovolskiy:** Resources (supporting). **Morris Lindner:** Resources (equal); Writing – review & editing (supporting). **Timmy Reimann:** Resources (equal); Writing – review & editing (supporting). **Carsten Dubs:** Resources (equal); Writing – review & editing (supporting). **Michal Urbánek:** Conceptualization (lead); Funding acquisition (equal); Project administration (supporting); Supervision (equal); Validation (lead); Writing – review & editing (equal). **Andrii V. Chumak:** Conceptualization (supporting); Funding acquisition (equal); Project administration (supporting); Supervision (lead); Writing – review & editing (equal).

DATA AVAILABILITY

The data that support the findings of this study are available from the corresponding author upon reasonable request.

REFERENCES

[1]A. Barman, G. Gubbiotti, S. Ladak, A. O. Adeyeye, M. Krawczyk, J. Grafe, C. Adelmann, S. Cotofana, A. Naeemi, V. I. Vasyuchka, B. Hillebrands, S. A. Nikitov, H. Yu, D. Grundler, A. V. Sadovnikov, A. A. Grachev, S. E. Sheshukova, J. Y. Duquesne, M. Marangolo, G. Csaba, W. Porod, V. E. Demidov, S. Urazhdin, S. O. Demokritov, E. Albisetti, D. Petti, R. Bertacco, H. Schultheiss, V. V. Kruglyak, V. D. Poimanov, S. Sahoo, J. Sinha, H. Yang, M. Münzenberg, T. Moriyama, S. Mizukami, P. Landeros, R. A. Gallardo, G. Carlotti, J. V. Kim, R. L. Stamps, R. E. Camley, B. Rana, Y. Otani, W. Yu, T. Yu, G. E. Bauer, C. Back, G. S. Uhrig, O. V. Dobrovolskiy, B. Budinska, H. Qin, S. Van Dijken, A. V. Chumak, A. Khitun, D. E. Nikonov, I. A. Young, B. W. Zingsem, and M. Winklhofer, "The 2021 magnonics roadmap," J. Phys.: Condens. Matter **33**, 413001 (2021).
[2]A. V. Chumak, P. Kabos, M. Wu, C. Abert, C. Adelmann, A. O. Adeyeye, J. Akerman, F. G. Aliev, A. Anane, A. Awad, C. H. Back, A. Barman, G. E. W. Bauer, M. Becherer, E. N. Beginin, V. A. S. V. Bittencourt, Y. M. Blanter, P. Bortolotti, I. Boventer, D. A. Bozhko, S. A. Bunyaev, J. J. Carmiggelt, R. R. Cheenikundil, F. Ciubotaru, S. Cotofana, G. Csaba, O. V. Dobrovolskiy, C. Dubs, M. Elyasi, K. G. Fripp, H. Fulara, I. A. Golovchanskiy, C. Gonzalez-Ballestero, P. Graczyk, D. Grundler, P. Gruszecki, G. Gubbiotti, K. Guslienko, A. Haldar, S. Hamdioui, R. Hertel, B. Hillebrands, T. Hioki, A. Houshang, C.-M. Hu, H. Huebl, M. Huth, E. Iacocca, M. B. Jungfleisch, G. N. Kakazei, A. Khitun, R. Khymyn, T. Kikkawa, M. Klaui, O. Klein, J. W. Klos, S. Knauer, S. Koraltan, M. Kostylev, M. Krawczyk, I. N. Krivorotov, V. V. Kruglyak, D. Lachance-Quirion, S. Ladak, R. Lebrun, Y. Li, M. Lindner, R. Macedo, S. Mayr, G. A. Melkov, S. Mieszczak, Y. Nakamura, H. T. Nembach, A. A. Nikitin, S. A. Nikitov, V. Novosad, J. A. Otalora, Y. Otani, A. Papp, B. Pigeau, P. Pirro, W. Porod, F. Porrati, H. Qin, B. Rana, T. Reimann, F. Riente, O. Romero-Isart, A. Ross, A. V. Sadovnikov, A. R. Safin, E. Saitoh, G. Schmidt, H. Schultheiss, K. Schultheiss, A. A. Serga, S. Sharma, J. M. Shaw, D. Suess, O. Surzhenko, K. Szulc, T. Taniguchi, M. Urbanek, K. Usami, A. B. Ustinov, T. van der Sar, S. van Dijken, V. I. Vasyuchka, R. Verba, S. V. Kusminskiy, Q. Wang, M. Weides, M. Weiler, S. Wintz, S. P. Wolski, and X. Zhang, "Advances in magnetics roadmap on spin-wave computing," IEEE Trans. Magn. **58**, 1–72 (2022).
[3]Y. Li, W. Zhang, V. Tyberkevych, W. K. Kwok, A. Hoffmann, and V. Novosad, "Hybrid magnonics: Physics, circuits, and applications for coherent information processing," J. Appl. Phys. **128**, 130902 (2020).
[4]O. V. Dobrovolskiy, R. Sachser, T. Brächer, T. Böttcher, V. V. Kruglyak, R. V. Vovk, V. A. Shklovskij, M. Huth, B. Hillebrands, and A. V. Chumak, "Magnon–Fluxon interaction in a ferromagnet/superconductor heterostructure," Nat. Phys. **15**, 477–482 (2019).
[5]Y. Tabuchi, S. Ishino, A. Noguchi, T. Ishikawa, R. Yamazaki, K. Usami, and Y. Nakamura, "Quantum magnonics: The magnon meets the superconducting qubit," C. R. Phys. **17**, 729–739 (2016).
[6]I. Boventer, M. Pfirrmann, J. Krause, Y. Schön, M. Kläui, and M. Weides, "Complex temperature dependence of coupling and dissipation of cavity magnon polaritons from millikelvin to room temperature," Phys. Rev. B **97**, 184420 (2018).
[7]V. A. Bittencourt, V. Feulner, and S. V. Kusminskiy, "Magnon heralding in cavity optomagnonics," Phys. Rev. A **100**, 013810 (2019).
[8]D. Lachance-Quirion, Y. Tabuchi, A. Gloppe, K. Usami, and Y. Nakamura, "Hybrid quantum systems based on magnonics," Appl. Phys. Express **12**, 070101 (2019).
[9]D. Lachance-Quirion, S. P. Wolski, Y. Tabuchi, S. Kono, K. Usami, and Y. Nakamura, "Entanglement-based single-shot detection of a single magnon with a superconducting qubit," Science **367**, 425–428 (2020).
[10]R. G. Morris, A. F. Van Loo, S. Kosen, and A. D. Karenowska, "Strong coupling of magnons in a YIG sphere to photons in a planar superconducting resonator in the quantum limit," Sci. Rep. **7**, 11511 (2017).
[11]B. Heinz, T. Brächer, M. Schneider, Q. Wang, B. Lägel, A. M. Friedel, D. Breitbach, S. Steinert, T. Meyer, M. Kewenig, C. Dubs, P. Pirro, and

27 July 2023 11:04:24

© Author(s) 2023

A. V. Chumak, "Propagation of spin-wave packets in individual nanosized yttrium iron garnet magnonic conduits," Nano Lett. **20**, 4220–4227 (2020).
[12]Q. Wang, M. Kewenig, M. Schneider, R. Verba, F. Kohl, B. Heinz, M. Geilen, M. Mohseni, B. Lägel, F. Ciubotaru, C. Adelmann, C. Dubs, S. D. Cotofana, O. V. Dobrovolskiy, T. Brächer, P. Pirro, and A. V. Chumak, "A magnonic directional coupler for integrated magnonic half-adders," Nat. Electron. **3**, 765–774 (2020).
[13]C. Dubs, O. Surzhenko, R. Linke, A. Danilewsky, U. Brückner, and J. Dellith, "Sub-micrometer yttrium iron garnet LPE films with low ferromagnetic resonance losses," J. Phys. D: Appl. Phys. **50**, 204005 (2017).
[14]C. Dubs, O. Surzhenko, R. Thomas, J. Osten, T. Schneider, K. Lenz, J. Grenzer, R. Hübner, and E. Wendler, "Low damping and microstructural perfection of sub-40nm-thin yttrium iron garnet films grown by liquid phase epitaxy," Phys. Rev. Mater. **4**, 024416 (2020).
[15]R. D. Henry, P. J. Besser, D. M. Heinz, and J. E. Mee, "Ferromagnetic resonance properties of LPE YIG films," IEEE Trans. Magn. **9**, 535–537 (1973).
[16]W. Hongxu and W. Wenshu, "The growth of LPE YIG films with narrow FMR linewidth," IEEE Trans. Magn. **20**, 1222–1223 (1984).
[17]Q. Wang, B. Heinz, R. Verba, M. Kewenig, P. Pirro, M. Schneider, T. Meyer, B. Lägel, C. Dubs, T. Brächer, and A. V. Chumak, "Spin pinning and spin-wave dispersion in nanoscopic ferromagnetic waveguides," Phys. Rev. Lett. **122**, 247202 (2019).
[18]L. Mihalceanu, V. I. Vasyuchka, D. A. Bozhko, T. Langner, A. Y. Nechiporuk, V. F. Romanyuk, B. Hillebrands, and A. A. Serga, "Temperature-dependent relaxation of dipole-exchange magnons in yttrium iron garnet films," Phys. Rev. B **97**, 214405 (2018).
[19]C. L. Jermain, S. V. Aradhya, N. D. Reynolds, R. A. Buhrman, J. T. Brangham, M. R. Page, P. C. Hammel, F. Y. Yang, and D. C. Ralph, "Increased low-temperature damping in yttrium iron garnet thin films," Phys. Rev. B **95**, 174411 (2017).
[20]S. Guo, B. Mccullian, P. C. Hammel, and F. Yang, "Low damping at few-K temperatures in $Y_3Fe_5O_{12}$ epitaxial films isolated from $Gd_3Ga_5O_{12}$ substrate using a diamagnetic $Y_3Sc_{2.5}Al_{2.5}O_{12}$ spacer," J. Magn. Magn. Mater. **562**, 169795 (2022).
[21]I. A. Golovchanskiy, N. N. Abramov, M. Pfirrmann, T. Piskor, J. N. Voss, D. S. Baranov, R. A. Hovhannisyan, V. S. Stolyarov, C. Dubs, A. A. Golubov, V. V. Ryazanov, A. V. Ustinov, and M. Weides, "Interplay of magnetization dynamics with a microwave waveguide at cryogenic temperatures," Phys. Rev. Appl. **11**, 044076 (2019).
[22]S. Kosen, A. F. Van Loo, D. A. Bozhko, L. Mihalceanu, and A. D. Karenowska, "Microwave magnon damping in YIG films at millikelvin temperatures," APL Mater. **7**, 101120 (2019).
[23]V. Vlaminck and M. Bailleul, "Spin-wave transduction at the submicrometer scale: Experiment and modeling," Phys. Rev. B - Condens. Matter Mater. Phys. **81**, 014425 (2010).
[24]M. Vaňatka, K. Szulc, O. Wojewoda, C. Dubs, A. V. Chumak, M. Krawczyk, O. V. Dobrovolskiy, J. W. Kłos, and M. Urbánek, "Spin-wave dispersion measurement by variable-gap propagating spin-wave spectroscopy," Phys. Rev. Appl. **16**, 054033 (2021).
[25]L. Temdie, V. Castel, C. Dubs, G. Pradhan, J. Solano, H. Majjad, R. Bernard, Y. Henry, M. Bailleul, and V. Vlaminck, "High wave vector non-reciprocal spin wave beams," AIP Adv. **13**, 025207 (2023).
[26]M. S. Alam, C. Wang, J. Chen, J. Zhang, C. Liu, J. Xiao, Y. Wu, L. Bi, and H. Yu, "Temperature control of spin wave propagation over 100 μm distance in 100 nm-thick YIG film," Phys. Lett. A **383**, 366–368 (2019).
[27]A. F. Van Loo, R. G. Morris, and A. D. Karenowska, "Time-resolved measurements of surface spin-wave pulses at millikelvin temperatures," Phys. Rev. Appl. **10**, 044070 (2018).
[28]D. Schmoll, "Enabling technology for high-frequency quantum magnonics," Master's thesis (University of Vienna, Wien, 2022).
[29]P. G. Baity, D. A. Bozhko, R. Macêdo, W. Smith, R. C. Holland, S. Danilin, V. Seferai, J. Barbosa, R. R. Peroor, S. Goldman, U. Nasti, J. Paul, R. H. Hadfield, S. McVitie, and M. Weides, "Strong magnon-photon coupling with chip-integrated YIG in the zero-temperature limit," Appl. Phys. Lett. **119**, 033502 (2021).
[30]H. Yu, O. D'Allivy Kelly, V. Cros, R. Bernard, P. Bortolotti, A. Anane, F. Brandl, R. Huber, I. Stasinopoulos, and D. Grundler, "Magnetic thin-film insulator with ultra-low spin wave damping for coherent nanomagnonics," Sci. Rep. **4**, 6848 (2014).
[31]S. S. Kalarickal, P. Krivosik, M. Wu, C. E. Patton, M. L. Schneider, P. Kabos, T. J. Silva, and J. P. Nibarger, "Ferromagnetic resonance linewidth in metallic thin films: Comparison of measurement methods," J. Appl. Phys. **99**, 093909 (2006).
[32]H. Chang, P. Li, W. Zhang, T. Liu, A. Hoffmann, L. Deng, and M. Wu, "Nanometer-thick yttrium iron garnet films with extremely low damping," IEEE Magn. Lett. **5**, 1–4 (2014).
[33]N. Loayza, M. B. Jungfleisch, A. Hoffmann, M. Bailleul, and V. Vlaminck, "Fresnel diffraction of spin waves," Phys. Rev. B **94**, 144430 (2018).
[34]J. Ding, T. Liu, H. Chang, and M. Wu, "Sputtering growth of low-damping yttrium-iron-garnet thin films," IEEE Magnetics Letters **11**, 5502305 (2020).
[35]O. A. Petrenko, D. M. K. Paul, C. Ritter, T. Zeiske, and M. Yethiraj, "Magnetic frustration and order in gadolinium gallium garnet," Phys. B: Condens. Matter **266**, 41–48 (1999).
[36]M. Sabbaghi, G. W. Hanson, M. Weinert, F. Shi, and C. Cen, "Terahertz response of gadolinium gallium garnet (GGG) and gadolinium scandium gallium garnet (SGGG)," J. Appl. Phys. **127**, 025104 (2020).
[37]B. A. Kalinikos and A. N. Slavin, "Theory of dipole-exchange spin wave spectrum for ferromagnetic films with mixed exchange boundary conditions," J. Phys. C: Solid State Phys. **19**, 7013–7033 (1986).
[38]P. Hansen, P. Röschmann, and W. Tolksdorf, "Saturation magnetization of gallium-substituted yttrium iron garnet," J. Appl. Phys. **45**, 2728–2732 (1974).
[39]I. V. Zavislyak and M. A. Popov, "Microwave properties and applications of yttrium iron garnet (YIG) films: Current state of art and perspectives," in *Yttrium: Compounds, Production and Applications* (Nova, 2009), pp. 87–126.
[40]M. J. Burek, Y. Chu, M. S. Liddy, P. Patel, J. Rochman, S. Meesala, W. Hong, Q. Quan, M. D. Lukin, and M. Loncar, "High quality-factor optical nanocavities in bulk single-crystal diamond," Nat. Commun. **5**, 5718 (2014).
[41]L. Wang, Z. Lu, X. Zhao, W. Zhang, Y. Chen, Y. Tian, S. Yan, L. Bai, and M. Harder, "Magnetization coupling in a YIG/GGG structure," Phys. Rev. B **102**, 144428 (2020).
[42]M. B. Jungfleisch, W. Zhang, W. Jiang, H. Chang, J. Sklenar, S. M. Wu, J. E. Pearson, A. Bhattacharya, J. B. Ketterson, M. Wu, and A. Hoffmann, "Spin waves in micro-structured yttrium iron garnet nanometer-thick films," J. Appl. Phys. **117**, 17D128 (2015).
[43]T. Liu, H. Chang, V. Vlaminck, Y. Sun, M. Kabatek, A. Hoffmann, L. Deng, and M. Wu, "Ferromagnetic resonance of sputtered yttrium iron garnet nanometer films," J. Appl. Phys. **115**, 17A501 (2014).
[44]M. Maryško, "Influence of GGG substrate on FMR and magnetostatic wave propagation," J. Magn. Magn. Mater. **101**, 159–161 (1991).

27 July 2023 11:04:24

© Author(s) 2023